Astron. Astrophys. 335, 341–350 (1998)

ASTRONOMY AND ASTROPHYSICS

The motion patterns of intranetwork magnetic elements

Jun Zhang[1], **Jingxiu Wang**[1], **Haimin Wang**[2], **and Harold Zirin**[3]

[1] Beijing Astronomical Observatory, Chinese Academy of Sciences, Beijing 100080, P.R. China (zhj@sun10.bao.ac.cn)
[2] Big Bear Solar Observatory, New Jersey Institute of Technology, USA
[3] Solar Astronomy, 264-33 Caltech, Pasadena, CA 91125, USA

Received 29 December 1997 / Accepted 27 March 1998

Abstract. By tracing individual elements, we have measured horizontal velocity and studied motion patterns of Intranetwork (IN) magnetic elements for the first time. The magnetograms obtained at Big Bear Solar Observatory span an interval of 10-hour and cover an area of 310×240 arc sec^2. In general, IN elements move radially and isotropically outwards from emergence centers to boundaries of supergranule cells at first. However, when they reach halfway between cell centers and boundaries, the motion of IN elements is non-isotropic, there are prior directions. Most of IN elements move towards the edges of network elements. There are two components of the velocity fields: radial velocity and circular velocity. From the centers to the boundaries of supergranule cells, the magnitude of the radial velocity decreases gradually; but that of the circular velocity increases obviously, at halfway between cell center and boundary, the circular acceleration reachs the maximum, about 10^{-1} m s^{-2}. The mean circular velocity near the boundary is about 0.4 km s^{-1}. The horizontal speeds deduced by tracing 768 intranetwork elements range from 0.05 km s^{-1} to 0.8 km s^{-1} with a peak distribution at 0.4 km s^{-1}. Both within the supergranule cells and on the boundaries, there are convergence centers, but divergence centers always exist within supergranule cells.

Key words: Sun: granulation – Sun: magnetic fields – Sun: photosphere

1. Introduction

Intranetwork (IN) magnetic fields were first observed by Livingston and Harvey (1975) and Smithson (1975). About a decade after the first discovery, the study of IN fields was suspended as the fields are very difficult to observe. In recent years progress was made in IN's morphology dynamics and some quantitative aspects from time sequence of deep magnetograms obtained at the Big Bear Solar Observatory (BBSO) (Livi et al. 1985; Martin 1984, 1988, 1990; Wang et al. 1985, 1988, 1995 [Paper 1]; Wang and Zirin 1988; Wang et al. 1996 [paper 2]; Zhang et al. 1997 [Paper 3], 1998 [Paper 4]; Zirin 1985, 1987, 1993). With spectroscopic techniques, it has been determined that IN fields are likely weak fields (comparing with the kilogauss network fields) (Keller et al. 1994; Lin 1995). Lites et al. (1996) presented recent observations of quiet regions near the center of the solar disk. These observations revealed horizontal magnetic flux structure, although most of the photospheric structures that they find are vertical.

The supergranule evolution patterns were first discovered by Hart (1954, 1956). They were named and studied extensively by Leighton et al. (1962) and Simon and Leighton (1964). The interaction between magnetic fields and convective flows on the sun has been a fundamental topic in solar physics (Spruit 1981; Parker 1982; Schmidt et al. 1985). More recently, with white light observations, some progresses were made on the cellular patterns of granulation and supergranule network (Schrijver 1997; Hirzberger et al. 1997). Hagenaar et al. (1997) found no significant dependence of cell size on local magnetic flux density.

In our previous papers, we presented some properties of IN elements on different aspects. Paper 1 described the flux distributions of quiet-Sun magnetic elements, IN flux ranges from 10^{16} Mx to 2×10^{18} Mx, with a peak distribution at 6×10^{16} Mx. Paper 2 derived mean horizontal velocity fields of IN and network fields by using the local correlation tracking techniques. In Paper 3, we estimated the lifetimes based on a sample of 528 IN elements, the lifetimes ranged from 0.2 hr to 7.5 hr with the mean of 2.1 hr. Paper 4 studied the evolution of IN magnetic elements, including the appearance and disappearance patterns, the interaction between IN and network elements.

In this paper, we will concentrate our study on horizontal velocity and motion patterns of IN elements. Although the velocity pattern has been given in Paper 2, that only represents mean flow averaged over the observing day. The magnetograms on June 4, 1992 are the best ever obtained for a quiet region at BBSO for the study of IN elements. The position was S10W3. The magnetograms were acquired by integrating 4096 video frames, and recording them in 16-bit memory. The 10-hour sequence consists of 83 images with an average temporal resolution of 7.2 minutes. The series of magnetograms have a gap of 35 minutes between 16:01 UT and 16:36 UT. From 15:47 UT to 19:44 UT, the seeing condition is very good, spatial resolution reach 1.5″, noise level is below 2 G. The pixel resolution is 0.6″ in the *X* direction and 0.5″ in the *Y* direction. The detection limit of magnetic flux is 10^{16} Mx, and the sensitivity of apparent flux density is 2 G. The calibration coefficient is 0.0122 G per pixel.

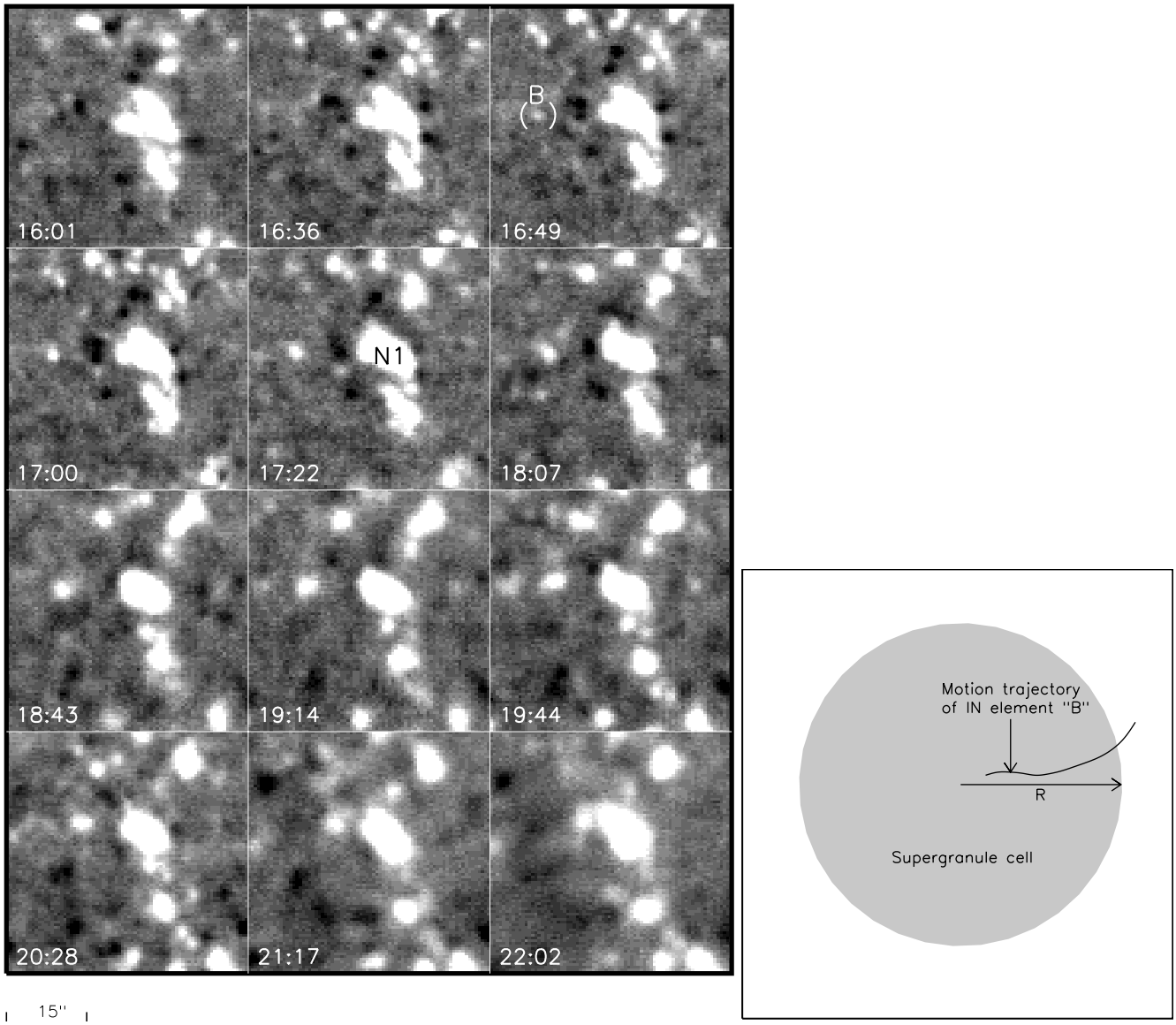

Fig. 1. a (left panel) The concentration of IN elements into network elements and interaction with each other. Almost all of the IN elements near the network element 'N1' move towards 'N1' and meet with it. At 16:49 UT, an IN element 'B' (in the brackets) of mixed polarities emerges and moves quickly to 'N1'. The peak speed, which occurred near 19:14 UT, is about 0.65 km s^{-1}. Finally, it merges with 'N1'. **b** (right panel) Motion pattern of IN element 'B'.

Additional information has been given in Papers 1, 2, 3, and 4. In Sect. 2, we give the velocity properties of IN elements, in Sect. 3, we present the collective behavior, Sect. 4 is the discussions.

2. Velocities of IN elements

2.1. Radial and circular velocity

The velocity fields of IN elements are very complicated. Almost all of IN elements move radially to the boundaries of supergranule cells. In Fig. 1a, we pay attention to a region of network boundary containing network elements. An IN element 'B' emerged at 16:49 UT moves quickly to a network feature 'N1'. Fig. 1b shows the motion trajectory of IN element 'B'. 'B' emerges near the center of supergranule cell, and moves mainly along the cell's radius although its motion trajectory is not a straight line. Table 1 lists the speed properties of 'B'.

In the table, 'D' is the motion distance, 'V' is mean speed of the interval, e.g., at the 33 minutes interval between 16:49 UT and 17:22 UT, 'B' moves 490 km, the mean speed is 0.25 km s^{-1}. From 16:49 to 22:02 UT, 'B' moves about 8×10^3 km, the mean speed is 0.42 km s^{-1}, the peak speed, which occurs near 19:14 UT, is about 0.65 km s^{-1} (see Table 1). During the proceeding of its migrating to network boundary, the flux increases prominently. Fig. 2a shows that IN element 'D' also moves along the cell's radius at first. In Fig. 3, the region in big circle at 15:47 UT indicates a very regular supergranule cell, most of IN elements ('A', 'B', 'D', 'E', 'F', 'G') in the cell

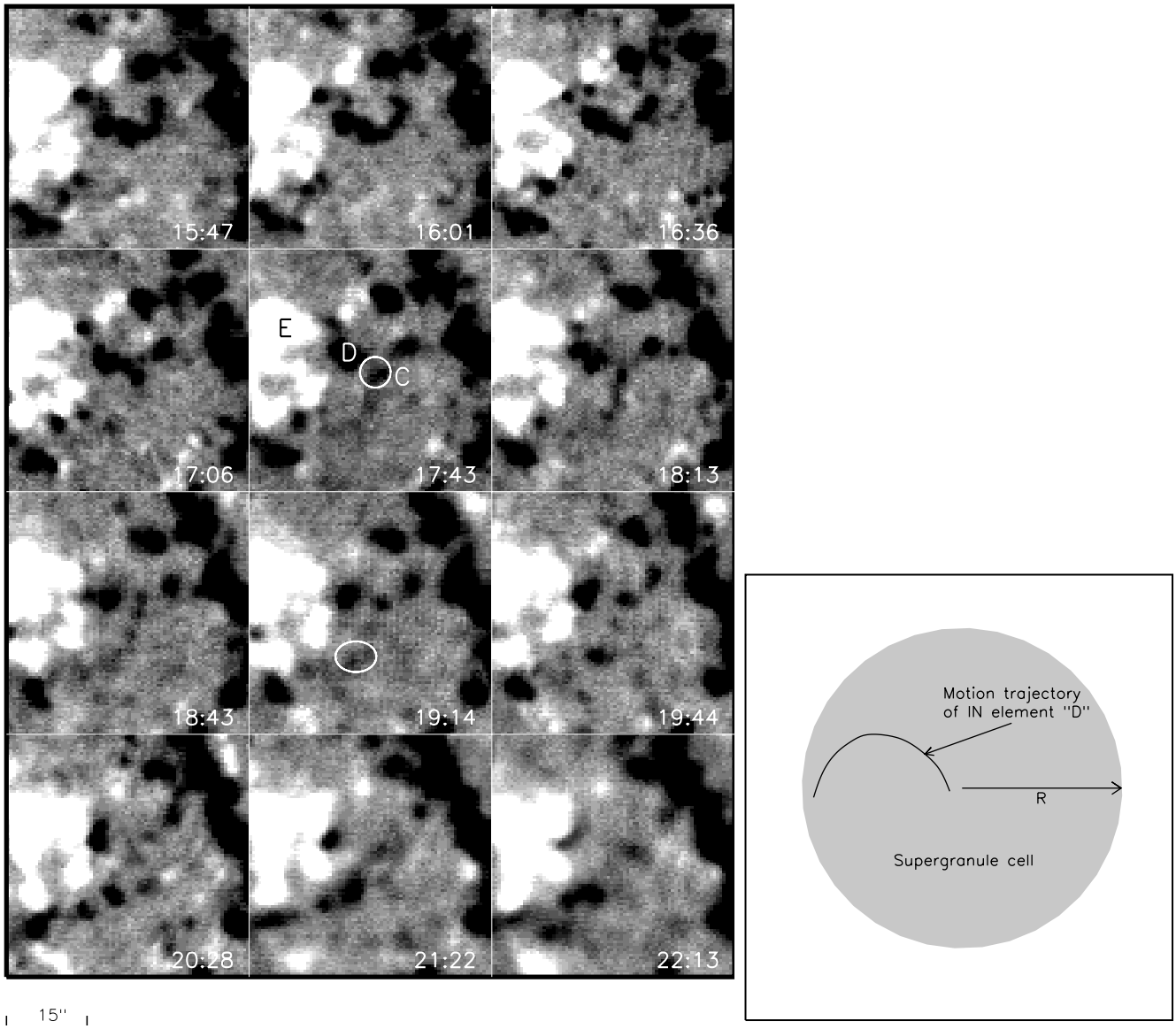

Fig. 2. a (left panel) Series of magnetograms at the site of a whole supergranule cell. 'D' moves along the radius of supergranule cell at first. When it reach the boundary of network element 'E', it changes the direction of motion, mainly moves along the edge of 'E' and cancels with it. 'C' splits into several smaller elements, these elements move outwards, the site of 'C' can be called a 'divergence center'. The site in the ellipse at 19:14 UT is a 'convergence center', IN elements beside the ellipse concentrate into it. **b** (right panel) Motion pattern of IN element 'D'.

move radially to the boundary of the cell. The fluxes of 'F' and 'G' change decreasingly and disappear before their arrival at the edge.

When IN elements reach halfway between cell centers and boundaries, especially when they near the cells boundaries, they change the motion direction and move across the radii of cells. Fig. 4 shows the motion of an IN element 'A' (in the brackets) near an opposite polarity network feature, 'A' moves along the edge of the network element. In Fig. 2a, we can see that after 'D' arrives at the boundary of the network element 'E', it does not cancel with the network element at once, furthermore, it moves predominantly downwards along the border of network element. Fig. 2b gives the motion pattern of 'D'. There is an obvious change of its motion direction and almost moves across the radius of supergranule cell.

The relationship between the radial (circular) velocities and normalized radius of supergranule cell is obtained by studying 208 IN elements within several regular supergranule cells in a particular interval. Fig. 5 gives the schematical sketch showing how to measure the radial and circular velocity. First, we choose a regular supergranule cell in the magnetograms, and determine the center(x0, y0) and the radius ($\sqrt{(x0-x)^2+(y0-y)^2}$) of the cell, at time t1, an IN element sits at the position (x1, y1),

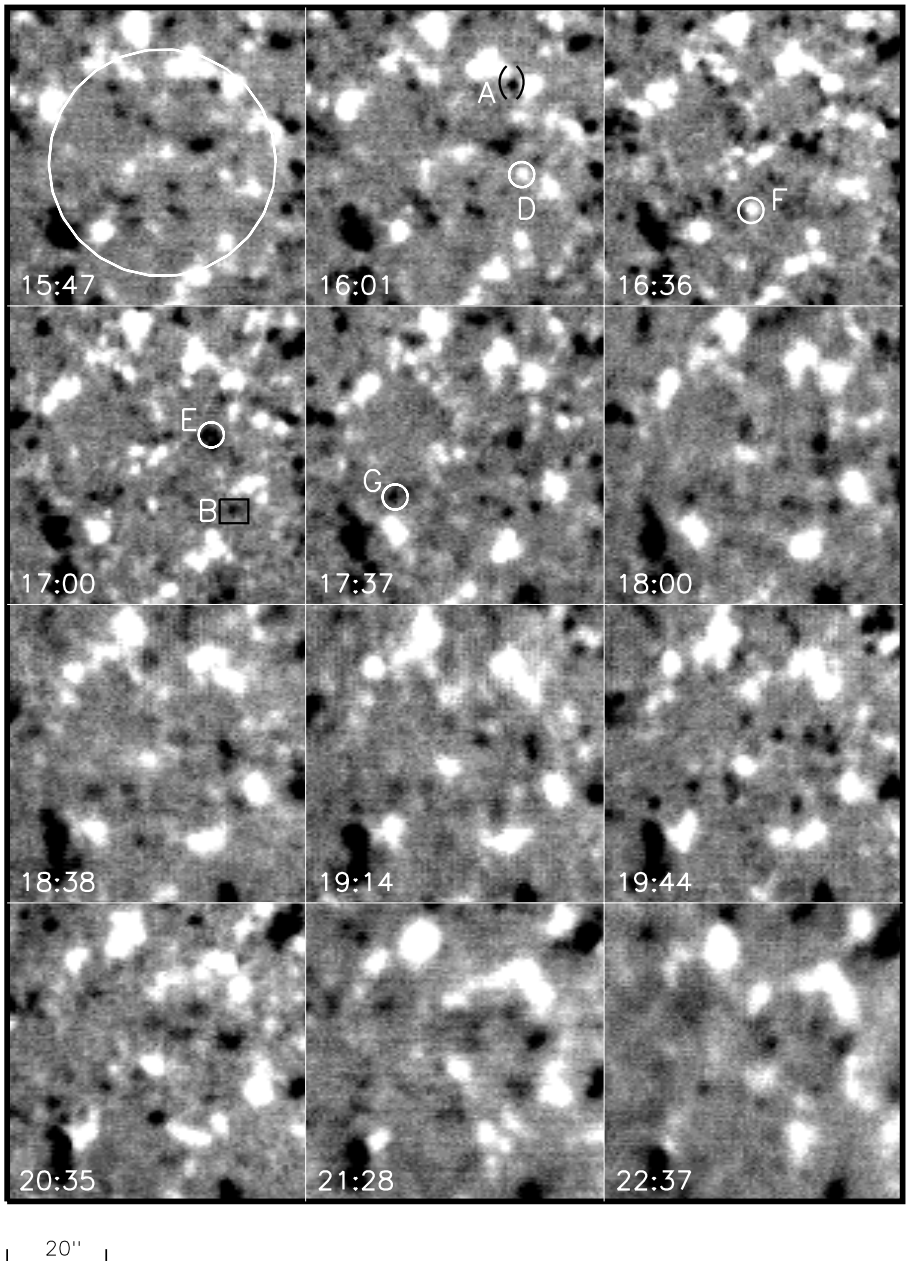

Fig. 3. Similarly to Fig. 2a. The region in big circle at 15:47 UT indicates a very regular supergranule cell. Almost all of the IN elements move radially to the boundary of the cell. The center of the supergranule cell can be considered a divergence center.

Table 1. Speed properties of 'B'

Time(UT)	D(km)	V(km s^{-1})
16:49 → 17:22	490	0.25
17:22 → 17:54	740	0.39
17:54 → 18:24	490	0.27
18:24 → 18:55	730	0.39
18:55 → 19:25	1170	0.65
19:25 → 19:56	740	0.40
19:56 → 20:28	1010	0.53
20:28 → 20:59	990	0.53
20:59 → 21:28	770	0.44
21:28 → 22:02	850	0.42

this position is represented by normalized radius of supergranule cell

$$r = \frac{\sqrt{(x0-x1)^2+(y0-y1)^2}}{\sqrt{(x0-x)^2+(y0-y)^2}} \quad (1)$$

Then at time t2, the element is at (x2, y2), we can obtain the radial position (x3, y3) from (x2, y2). The radial velocity is defined as

$$v_r = \frac{\sqrt{(x3-x1)^2+(y3-y1)^2}}{t2-t1} \quad (2)$$

and the circular velocity is

$$v_c = \frac{\sqrt{(x3-x2)^2+(y3-y2)^2}}{t2-t1} \quad (3)$$

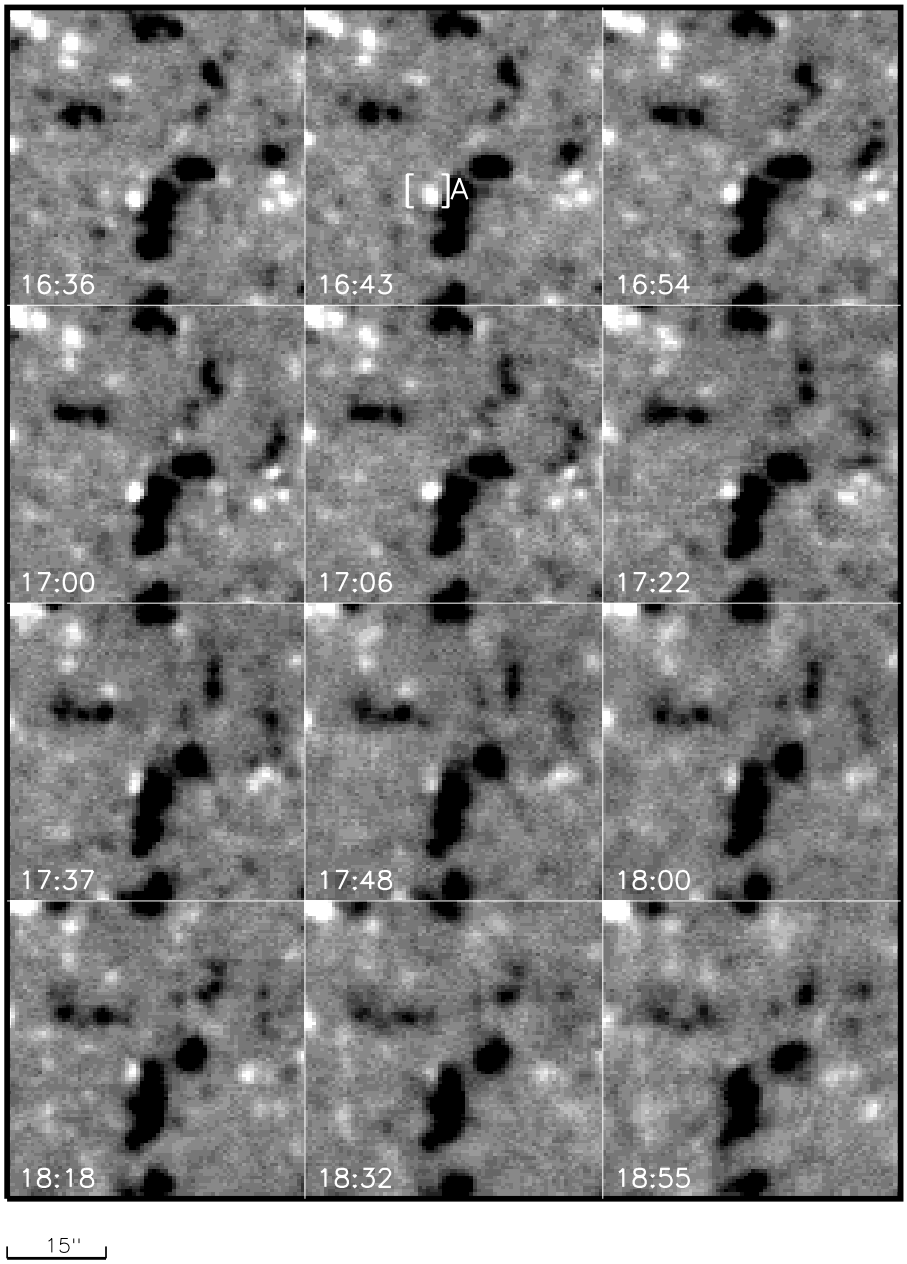

Fig. 4. Series of magnetograms showing the motion of IN element 'A' around boundary of a network element.

The interval (t2−t1) we choose is 18 minutes (t2=16:54 UT, t1=16:36 UT) although the temporal resolution of the magnetograms is 6 minutes between 16:36 and 19:44 UT, because the longer the interval, the smaller the error ($\sim$(t2−t1)$^{-1}$). In order to obtain the velocity fields of IN elements in supergranule cells, we track 10 IN elements which emerge near the centers of cells and move towards the boundaries. We have measured the radial and circular velocities corresponding to normalized radius in different interval. Fig. 6 shows the relationship between radial velocity and normalized radius. The upper panel gives the radial velocity of 208 IN elements in the interval between 16:36 UT and 16:54 UT, and the lower panel shows the radial velocity of the 10 elements traced in different interval, each interval is also about 18 minutes. We label the velocity of each element by a particular symbol. We can see that, from the centers to boundaries of supergranule cells, the magnitude of the mean radial velocity decreases slightly. Similarly to Fig. 6, Fig. 7 gives the relationship between circular velocity and normalized radius, we find the mean circular velocity increase predominantly from center to boundary, and near the boundary, the mean circular velocity is 0.4 km s^{-1}.

2.2. Mean horizontal speed

The horizontal speed of IN elements was derived with standard local correlation tracking techniques (November 1986; Wang and Zirin 1988, and Paper 2). This speed is a lower limit of the true speed of supergranules as there are certain areas on the quiet Sun which do not have observable magnetic fields at a particular time, the local correlation tracking would find zero speed for

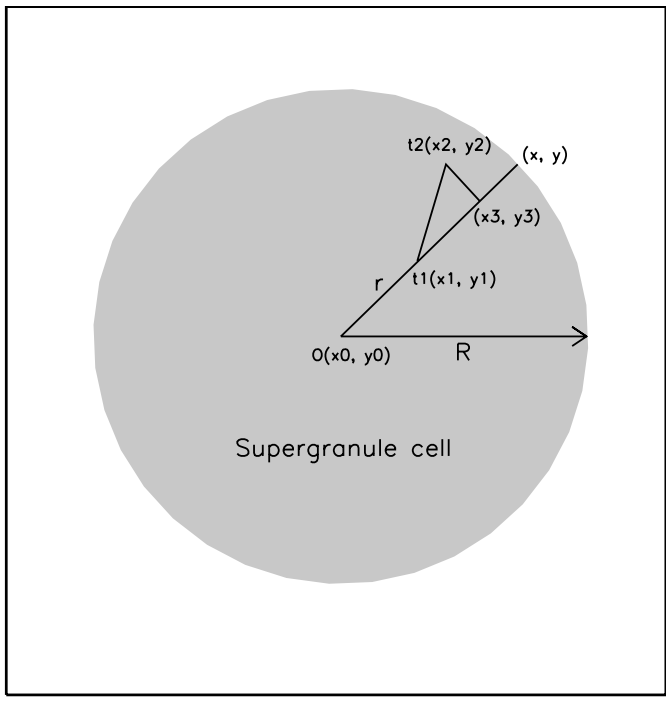

Fig. 5. Schematical sketch showing how to measure the radial and circular velocity. At time t1, an IN element sits at the position (x1, y1); then at time t2, the element is at (x2, y2). We can deduce the radial position (x3, y3) from (x2, y2), the radial velocity is $\sqrt{(x3-x1)^2+(y3-y1)^2}(t2-t1)^{-1}$, and the circular velocity is $\sqrt{(x3-x2)^2+(y3-y2)^2}(t2-t1)^{-1}$.

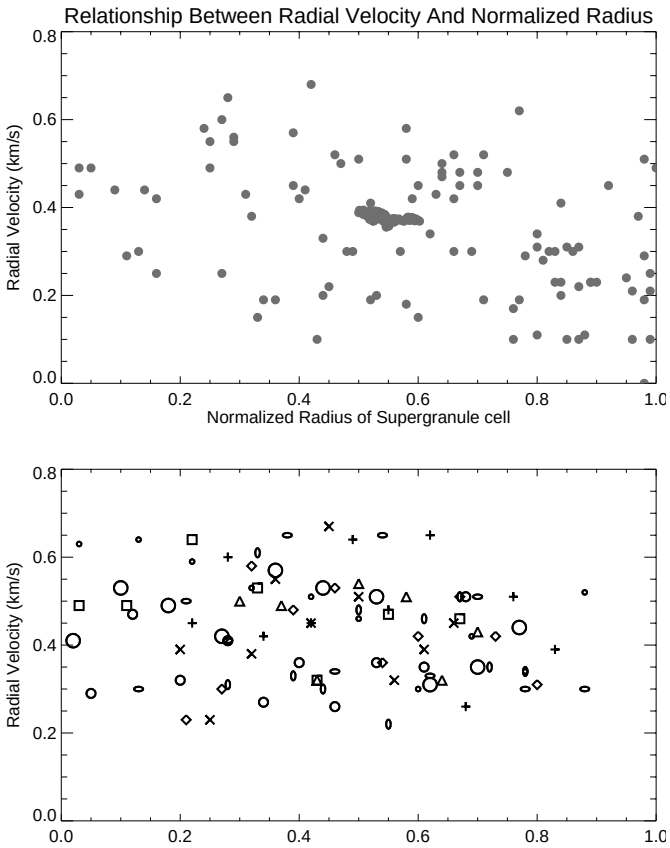

Fig. 6. Plots showing the relationship between radial velocity and normalized radius of supergranule cell. Upper panel: radial velocity of 208 IN elements in the interval between 16:36 UT and 16:54 UT; lower panel: radial velocity of 10 IN elements in different interval, each interval is also about 18 minutes. We label the velocity of each element by a particular symbol.

these regions, while the true supergranular speeds are not zero. November (1994) have deduced the vertical velocity of supergranule cells form Doppler measurements. From the 10-hour sequence of observations, we are able to deduce the horizontal speed by tracing 768 intranetwork elements. The speed of each element is obtained by measuring the motion distance of the element in a particular interval, the interval usually is about 30 minutes. We choose the interval between 16:36 UT and 17:06 UT and have measured the speeds of 520 IN elements. In order to enlarge the sample, we choose another interval between 19:44 and 20:16 UT, and the speeds of 248 IN elements are obtained. Fig. 8 shows a histogram of speeds of these elements. the speeds range from 0.05 km s^{-1} to 0.8 km s^{-1} with a peak distribution at 0.4 km s^{-1}.

The velocity measurement may have some error, because the measurement of position is not very precise. We consider the position error is one pixel, the error of radial and circular velocity is (one pixel)$(t2-t1)^{-1}$. As the size of one pixel is about 0.30″ (we enlarge the magnetograms while we measure the velocity fields) and t2−t1 is 18 minutes, the error equals 0.20 km s^{-1}. The mean horizontal speed is obtained by tracing 768 IN elements in two interval of 30 minutes, the error of mean horizontal speed is close to 0.10 km s^{-1}, which is smaller than that of radial and circular velocity.

3. Collective behavior of IN elements

3.1. Divergence centers and convergence centers

From the series of magnetograms, we find within a supergranule cell, some IN elements move outwards from a region, this region can be called ‘divergence center’. In Fig. 2a, a divergence center is shown. All the IN elements near the region ‘C’ depart from ‘C’. At 20:28 UT, the IN elements at ‘C’ disappear. We can see clearly that, in Fig. 3, most of IN elements move radially to the boundary of the cell, the center of the supergranule cell also can be considered a divergence center. We have noticed that divergence centers do not exist on boundaries of supergranule cell. Divergence centers may represent the site of upflows of supergranule, the flow drives the flux of IN elements onto the solar photosphere, then pushes the IN elements outwards to the boundary of supergranule cell (Paper 2).

Opposite to divergence center, convergence center gives another view: flow of supergranule assembles IN elements together. In Fig. 1a, almost all of the IN elements near the network element ‘N1’ move towards ‘N1’ and meet with it, the site of ‘N1’ is a convergence center. Fig. 9 gives another example of convergence center, we keep our eyes open on the magnetic el-

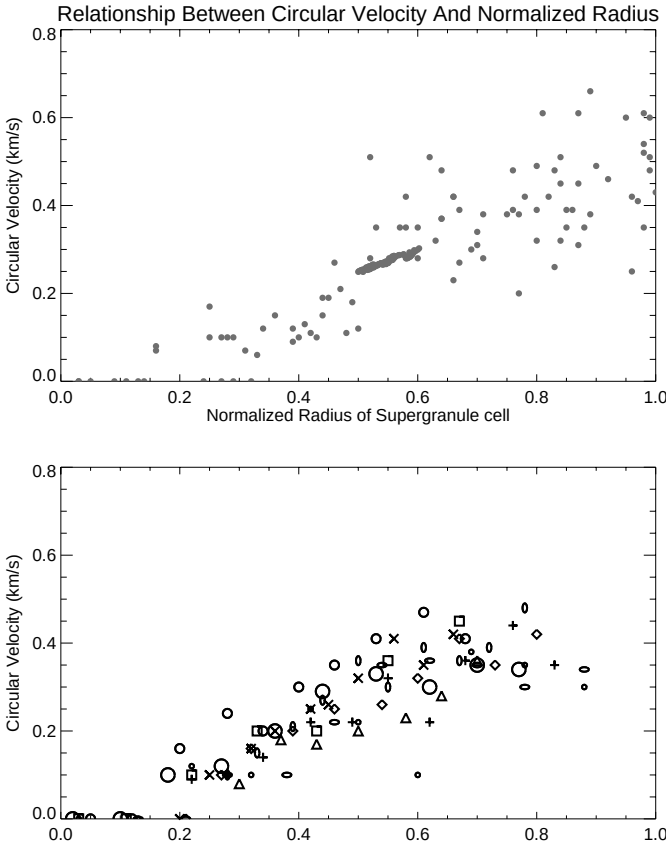

Fig. 7. Similarly to Fig. 6. Plots showing the relationship between circular velocity and normalized radius of supergranule cell. Upper panel: circular velocity of 208 IN elements in the interval between 16:36 UT and 16:54 UT; lower panel: circular velocity of 10 IN elements in different interval, each interval is also about 18 minutes. We label the velocity of each element by a particular symbol.

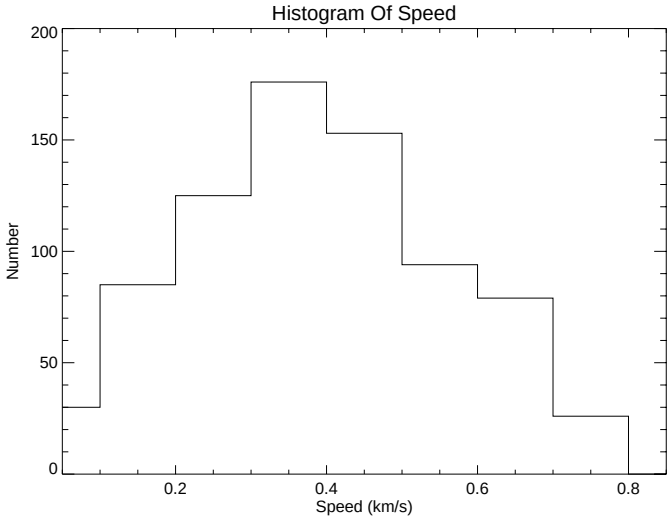

Fig. 8. The histogram showing the distribution of intranetwork elements speed.

ements in the region of the square (signed at 16:36 UT). In this region, most of the elements move to the locality in the circle (labelled at 16:54 UT). Usually convergence center is located on the boundaries of supergranules, but there are exceptions. Within supergranule cells, we also find a concentration center, Fig. 2a gives an example, we mark the site with an ellipse at 19:14 UT. IN elements beside the ellipse concentrate into it at 22:13 UT and form another IN element with larger amount of flux.

3.2. Velocity mappings

The velocity patterns of the IN elements were derived with local correlation tracking techniques (Wang and Zirin 1988, also Paper 2). Brandt et al. (1988) reported a vortex structure which visibly dominates the motion of the granules in its neighbourhood. In using of this series of magnetograms, we have summarised some velocity patterns of IN elements. Fig. 10a is a mapping of velocity about IN elements. We choose a region of the boundary of several supergranulars. I, II, III, IV show the supergranule cells, letters 'a,b, ... p' signed in the supergranule cells express IN elements, 'N1' and 'N2' are network elements, the lengths of arrows are the sizes of speed, and their directions mean that of motion. All of IN elements except 'd', 'i', 'j' move towards two regions 'C1' and 'C2' just nearby two network elements, we call 'C1' and 'C2' concentration centers. 'N2' also moves to region 'C1'. According to the measurement of speed in Sect. 2, the peak speed, which usually occurs halfway between the cell centers and the boundaries, is about 0.80 ± 0.10 km s^{-1}. The r.m.s. speed is 0.40 ± 0.10 km s^{-1}. These speeds are larger than the values derived from the Doppler measurements (peak speed: 0.5 km s^{-1}; r.m.s. speed: 0.3 km s^{-1}, see Wang 1988).

Fig. 10b gives another velocity mapping. We consider a region of supergranule cell. Similarly to Fig. 10a, most of IN elements move towards some particular sites in the neighbourhood of network elements. However, this Fig. gives additional information: at the center of supergranule cell there is an emergence center 'M', dipole magnetic features (or ephemeral regions, 'm1' and 'm2') emerged nearby 'M' move radially outwards at first, then the dipole magnetic feature separate each other and change the direction of motion, specially move across the radius of supergranule. The edges of most network elements ('M1', 'M2', 'M4', 'M5') are the concentration centers but there is exception ('M3').

From the mappings above, we simplified the motion patterns of IN elements as following: most of IN elements move radially and isotropically outwards from emergence centers to boundaries of supergranule cells at first. However, when they reach halfway between cell center and boundaries, the motion of IN elements is non-isotropic, there are preferred directions. Most of IN elements move towards the edges of network elements and merge (or cancel) with network features. During the proceeding of their migrating to network boundary, the fields of some elements become stronger and stronger and can arrive at the edge. On the other hand, others become weaker and weaker, and some of them disappear inside the cells before they arrive at the boundary.

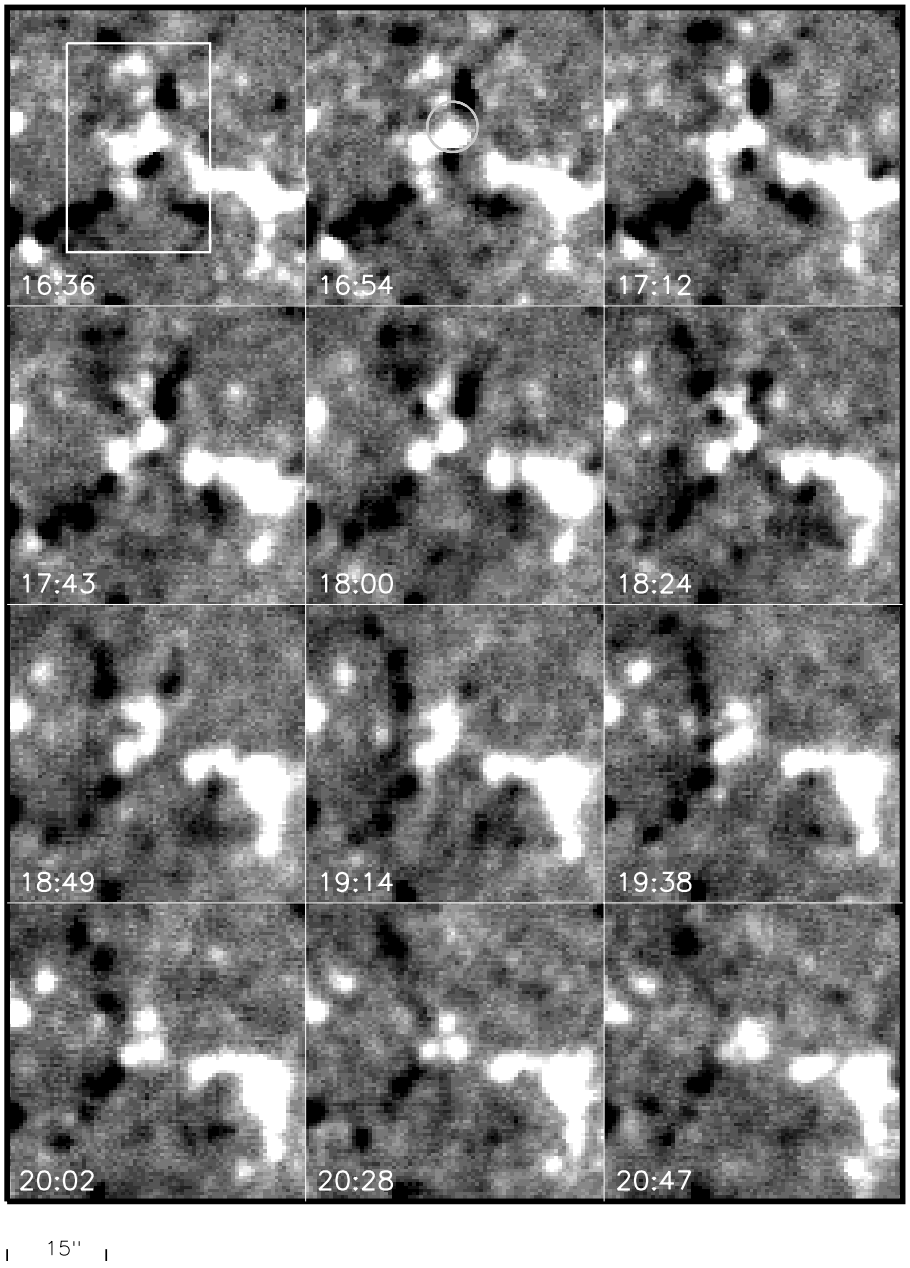

Fig. 9. Series of magnetograms showing the concentration. Most of the magnetic elements in the region of square (signed at 16:36 UT) move to the locality in the circle (labelled at 16:54 UT).

4. Discussions

We find an original motion of magnetic elements towards the supergranule boundary with a circular velocity. This indicates that some helicity does exist in the supergranule. The observations come from the south hemisphere and we observe mainly some counterclockwise motion. May be the motion of these small magnetic elements belong to the large scall velocity pattern on the Sun. There are two components of the velocity fields, radial velocity and circular velocity. We try to estimate the Coriolis force, $F_c = 2\rho v_r \times \frac{v_c}{D}$, resulted from the velocity fields, where ρ is mass density on the photosphere, *D* is radius of supergranule cell. $D \sim 10^7$ m, $\rho \sim 10^{-4}$ kg m^{-3}, v_c, $v_r \sim 5 \times 10^2$ m s^{-1}. The Coriolis force is on the order of 10^{-5} N m^{-3}.

In general, the motion of IN magnetic elements follows the supergranule patterns, the mean horizontal speed represents that of supergranule outflow. However, we should point out that the motion patterns of IN elements may be affected by some other factors: IN elements with larger flux may move under its buoyancy force, e.g., the ephemeral regions separate at about 0.6 km s^{-1} (Zirin 1985), regardless of the local flow; Berger and Title (1996) reported that motions of small-scale magnetic flux appeared to be constrained to the intergranule lanes and were primarily driven by the evolution of the local granule convection flow fields. Figs. 6 and 7 tell us the velocity fields of IN elements are very complicated. From centers of supergranule cells to boundaries, the magnitude of radial velocity decreases slightly, but that of circular velocity increases substantially. If we take the radius of a supergranule cell as 10^4 km, at halfway be-

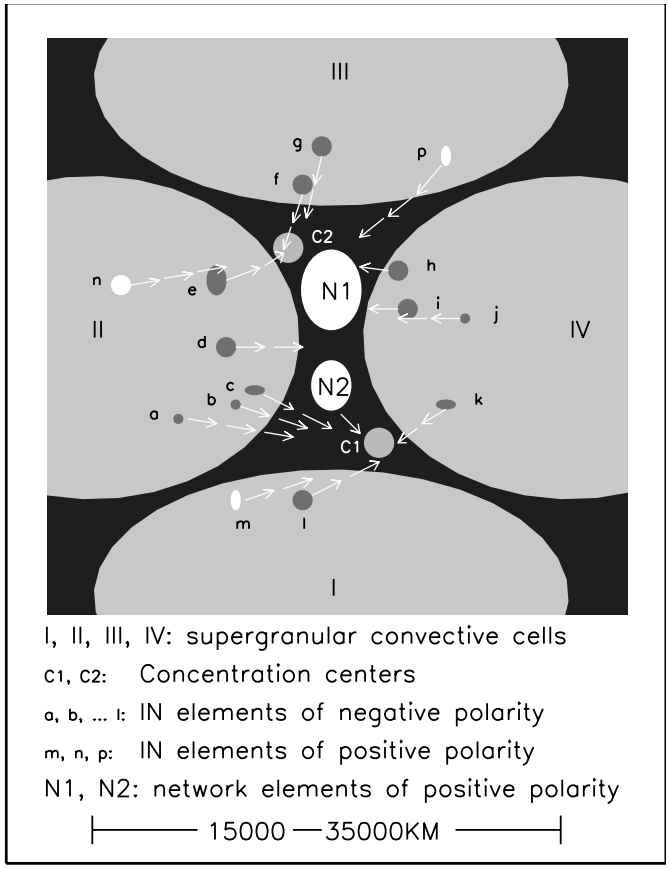

Fig. 10a. A velocity mapping of IN elements in the region of the boundaries of several supergranule cells. I, II, III, IV show the supergranule cells, letters 'a,b, ... p' signed in the supergranule cells express IN elements, 'N1' and 'N2' are network elements, the lengths of arrows are the sizes of speed, and the direction of arrows mean that of motion. All of IN elements except 'd', 'i', 'j' move towards two regions 'C1' and 'C2' just nearby two network elements, we call 'C1' and 'C2' the concentration centers. 'N2' also moves to region 'C1'. The peak speed, which usually occurs halfway between the cell center and the boundary, is about 0.8 ± 0.10 km s^{-1}. The r.m.s. speed is 0.40 km s^{-1}.

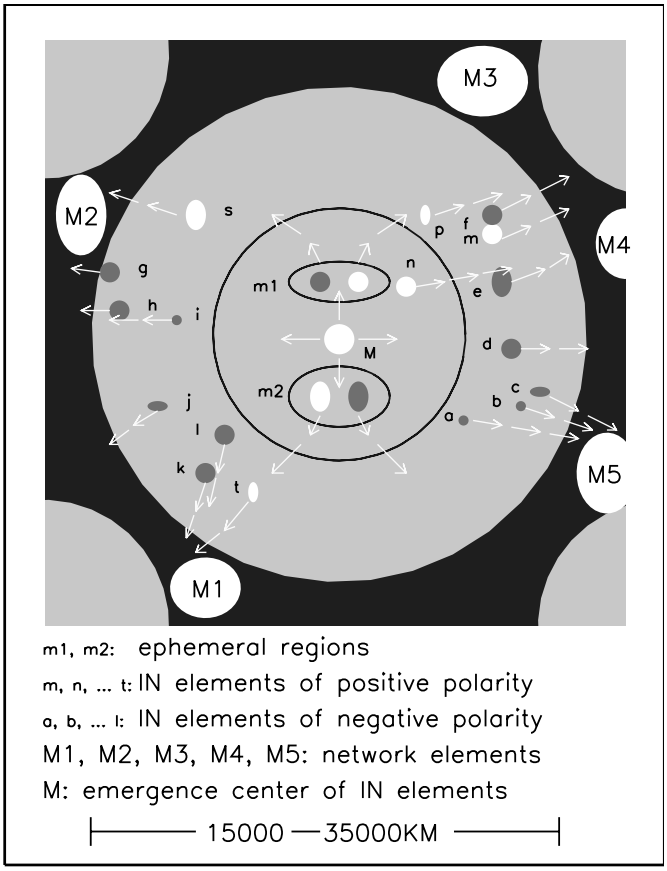

Fig. 10b. A velocity mapping of IN elements in a supergranule cell. Similarly to Fig. 10a, most of IN elements move towards some particular sites in the neighbourhood of network elements. At the center of supergranule cell there is an emergence center 'M', dipole magnetic features (or ephemeral regions, 'm1' and 'm2') emerge nearby 'M' and move radially outwards at first, then the dipole magnetic feature separate each other and change the direction of motion, specially move across the radius of supergranule. The edges of most network elements ('M1', 'M2', 'M4', 'M5') are the concentration centers but there is exception ('M3').

tween cell center and boundary, the circular acceleration reachs the maximum, about 0.1 m s^{-2}. We suggest that the motion patterns of IN elements are mainly determined by large-scale supergranule draft, small-scale granule flow, and the interaction between IN and network magnetic fields. Supergranule draft tends to sweep IN elements from the inside of supergranule cell to the boundaries, while granule flow and the interaction of IN and network magnetic fields give some modulation to the overall motion patterns of IN elements.

An additional consequence of the dynamic behavior of IN elements we observe in the magnetograms is the creation of large currents caused by evolution of magnetic fields. As a simple estimate of the current density caused by merging of two same polarity magnetic elements (i.e., in Fig. 1a, 'B' merges with 'N1'), we model the elements as solenoids, vertically oriented in the photosphere. We assume the diameter of each solenoid is 200 km, the field strength is 1000 G and is uniformly across the area of the element. Let one element merges with the other element after moving a distance greater than 200 km with a speed of 0.4 km s^{-1} and forms another element. Consider a circuit closely enclosing the formed element, the conductivity is 100A m^{-1} in the lower photosphere (Kopecký & Soytüry 1971), an azimuthal current density on the order of 10^3 A m^{-2} is induced in the circuit. As the nature of the conductivity is complex in the convective plasma of the photosphere, actual current density induced by such merging is expected to be lower than that calculated above. Hirayama (1992) calculated an azimuthal current density in a thin flux tube model on the order of 100 A m^{-2}.

Resent studies of the emergence of magnetic flux tubes revealed the non-potential nature of magnetic fields (e.g., Wang 1994). The flux tubes are twisted before their emergence on the photosphere. From the motion patterns of IN elements, we can

deduce the electric currents associated with the twist fields. We consider magnetic elements as twist flux tubes,

$$\mathbf{B} = \mathbf{B}_z + \mathbf{B}_\psi \tag{4}$$

where $\mathbf{B}_z$ and $\mathbf{B}_\psi$ are the axis and azimuthal components of magnetic flux density. The currents caused by $\mathbf{B}_\psi$ is parallel to $\mathbf{B}_z$. We have mentioned above that after IN elements meet with network elements, usually IN elements move along the peripheries of network elements for some distance, this phenomenon may be caused by the vertical currents interaction between IN and network elements. As a simple estimate of the vertical current density, we consider IN and network elements as the same solenoids (equal area, equal field strength). IN element moves along network element with a speed of 0.4 km s^{-1}, the centripetal force of moving IN element is provided by electromagnetic force. The magnitude of vertical current density can be derived from motion equation:

$$\rho\frac{v^2}{R} \simeq J \times B_\psi \tag{5}$$

as:

$$B_\psi = \frac{\mu_0 I}{2\pi R} \tag{6}$$

$$I = \pi R^2 J \tag{7}$$

Consequencely, Eq. (5) reads

$$\rho\frac{v^2}{R} \simeq \frac{1}{2}\mu_0 R J^2 \tag{8}$$

where ρ is internal mass density, *v* is speed of IN element, *R* is the radius of network element, *I*, *J* and B_ψ are vertical current, vertical current density, and azimuthal field strength, respectively.
$\rho = 3.3 \times 10^{-4}$ kg m^{-3}
$v = 400$ m s^{-1}
R = 10^5 m
We derived a vertical current density on the order of 10^{-1} A m^{-2} and a corresponding azimuthal field strength B_ψ of 10^2 G in a twist magnetic flux tube. Previous studies have indicated that current systems within flux tubes may have very significant effects on the gasdynamics within and immediately outside flux tubes (Hirayama 1992; Henoux & Somov 1994).

Acknowledgements. We would like to thank the referee, Dr. B. Schmieder, for valuable comments and useful suggestions. This work is supported by the Major Project 19791090, funded by National Natural Science Foundation of China (NSFC), US NSF CAREER Award ATM-9628862 to Wang and NSF China-US collaboration grant INT-9603534.

References

Berger T.E., Title A.M., 1996, ApJ 463, 365
Brandt P.N., 1988, Nature 335, 238
Hagenaar H.J., Schrijver C.J., Title A.M., 1997, ApJ 481, 988
Hart A.B., 1954, Monthly Notice of Roy. Astro. Soc. 114, 2
Hart A.B., 1956, Monthly Notice of Roy. Astro. Soc. 116, 38
Henoux J.C., Somov B.V., 1994, in Solar Active Region Evolution: Comparing Model with Observations. Vol, 68, ed. K. S. Balasubramaniam and G. W. Simon (San Francisco: ASP), 158
Hirayama T., 1992, Solar Phys. 137, 33
Hirzberger J., Vázquez M., Bonet J., Hanslmeier A., Sobotka, M., 1997, ApJ 480, 406
Keller C.J., Deubner F.L., Egger U., Fleck B., Povel H.P., 1994, A&A 286, 626
Kopecký M., Soytürk E., 1971, Bull. Astron. Inst. Czechoslovakia, 22, 154
Leighton R.B., Noyes R.W., Simon G.W., 1962, ApJ 135, 474
Lin H., 1995, ApJ 446, 421
Lites B.W., Leka K.D., Skumanich A., Martínez Pillet V., Shimizu T., 1996, ApJ 460, 1019
Livi S.H.B., Wang J., Martin S.F., 1985, Australian J. Phys. 38, 855
Livingston W.C., Harvey J., 1975, Bull. Amer. Astron. Soc. 7, 346
Martin S.F., 1984, in Small-Scale Dynamical Processes in Quiet Stellar Atmospheres, ed. S.L.Keil, p. 30, Sunspot, NM
Martin S.F., 1988, Solar Phys. 117, 243
Martin S.F., 1990, in Solar Photosphere: Structure, Convection and Magnetic Fields, ed. Stenflo, p. 129
November L., 1986, Appl. Optics 25, 392
November L., 1994, Solar Phys. 151, 1
Parker E.N., 1982, ApJ 256, 746
Schmidt H.U., Simon G.W., Weiss N.O., 1985, A&A 148, 191
Schrijver C.J., Hagenaar H.J., Title A.M., 1997, ApJ 475, 328
Simon G.W., Leighton R.B., 1964, ApJ 140, 1120
Smithson R.C., 1975, Bull. Amer. Astron. Soc. 7, 346
Spruit H.C., 1981, A&A 98, 155
Wang H., 1988, Solar Phys. 117, 343
Wang H., Tang F., Zirin H., Wang J., 1996, Solar Phys. 165, 223 (Paper 2)
Wang H., Zirin H., 1988, Solar Phys. 115, 205
Wang J., Zirin H., Shi Z., 1985, Solar Phys. 98, 241
Wang J., Shi Z., 1988, Acta Astron. Sinica 29, 48
Wang J., 1994, Solar Phys. 155, 285
Wang J., Wang H., Tang F., Lee J.W., Zirin H., 1995, Solar Phys. 160, 277 (Paper 1)
Zhang J., Lin G., Wang J., Wang H., Zirin H., 1997, accepted by Solar Phys. (Paper 3).
Zhang J., Lin G., Wang J., Wang H., Zirin H., 1998, submitted to A&A (Paper 4)
Zirin H., 1985, Australian J. Phys. 36, 961
Zirin H., 1987, Solar Phys. 110, 101
Zirin H., 1993, in Magnetic and Velocity Fields of Solar Active Regions, eds Zirin, Ai and Wang, p. 215